

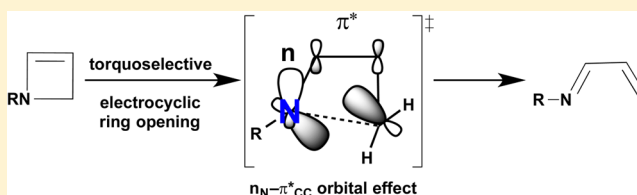
# Substituent Effects on Rates and Torquoselectivities of Electrocyclic Ring-Openings of *N*-Substituted 2-Azetines

Steven A. Lopez and K. N. Houk\*

Department of Chemistry &amp; Biochemistry, University of California, Los Angeles, California 90095-1569, United States

## S Supporting Information

**ABSTRACT:** Transition structures for the conrotatory electrocyclic ring-opening reactions of *N*-substituted 2-azetines were computed with the density functional M06-2X/6-31+G(d,p). A wide range of substituents from  $\pi$  acceptors (e.g., CHO, CN) to  $\pi$  donors (NMe<sub>2</sub>, OMe) was explored. Acceptor substituents delocalize the nitrogen lone pair and stabilize the reactant state of 2-azetines, while donors destabilize the 2-azetine reactant state. The conrotatory ring-opening is torquoselective, and the transition state for the outward rotation of the *N*-substituent and inward rotation of the nitrogen lone pair is preferred. This transition structure is stabilized by an interaction between the nitrogen lone pair and the vacant  $\pi^*$  orbital. The activation free energies are linearly related to the reaction free energies and the Taft  $\sigma_R^0$  parameter.



## INTRODUCTION

Cyclobutenes undergo thermal conrotatory  $4\pi$  electrocyclic ring-opening reactions to afford 1,3-butadienes.<sup>1</sup> Substituents may rotate “inward” or “outward” in their reactions. A preference for one diastereomeric transition state is called torquoselectivity.<sup>2</sup> The term was coined in the 1980s because ring-opening involves twisting or torque of the breaking single bond. This selectivity has been shown to arise from interactions between the substituent orbitals and those of the breaking bond. Donors rotate outward to avoid repulsive filled–filled interactions with the HOMO of cyclobutene upon inward rotation. Acceptors have low-lying vacant orbitals, and the best acceptors (CHO,  $-\text{SiR}_3$ ,  $\text{GeR}_3$ ) preferentially rotate inward.

Our group published DFT calculations on the torquoselectivities of 2-azetines (also known as 1,2-dihydroazete) and carbocyclic derivatives. The N–H greatly prefers to rotate outward, while the nitrogen lone pair rotates inward (Scheme 1).<sup>3</sup> This preference results from an interaction of the nitrogen lone pair with the azetine  $\pi^*$  (LUMO) orbital in the transition state upon inward rotation of the nitrogen lone pair. The other mode of conrotatory ring-opening has the *N*-substituent rotating inward and nitrogen lone pair rotating outward. This diminishes interaction of the lone pair with the  $\pi^*$  orbital. Chattaraj et al. published DFT calculations on the electrocyclic ring-opening reaction rates of related heterocyclic unsaturated four-membered rings, including unsubstituted 2-azetines.<sup>4</sup> They also report a strong preference for the outward rotation of heteroatom substituents and inward rotation of the heteroatom lone pair. This was explained using activation hardness theory<sup>5</sup> ( $\Delta n^\ddagger$ ), which analyzes reactivity based on the energy change of frontier molecular orbitals from reactant to transition state. De Kimpe et al. studied the ring-opening reaction of various 3-chloro-2-azetines experimentally and with DFT calculations. They established that aryl groups at the 4-position stabilize the

transition states and result in significantly more facile ring-opening reactions.<sup>6</sup> Scheme 1 shows the possible products upon ring-opening and a diagram of the frontier molecular orbital interactions for both modes of conrotatory ring-opening transition structures.

We have explored how *N*-substituents affect the conversion rate of 2-azetines to 1-azadienes. The 1-azadienes are electron-deficient and can participate in hetero-Diels–Alder cycloadditions with inverse-electron-demand. This cycloaddition is the key step in the synthesis of many heterocyclic targets<sup>7</sup> such as  $\delta$ -coniceine<sup>8</sup> and piericidin A1 and B1<sup>9</sup> (Scheme 2). The 1-azadienes have been shown to react regio- and chemoselectively in asymmetric (4 + 2), (3 + 2), and (2 + 2) cycloadditions as  $2\pi$  or  $4\pi$  components.<sup>10</sup> Relatively stable 2-azetines have *N*-substituents that are strong  $\pi$  acceptors. Jung<sup>8</sup> and Bott<sup>11</sup> report syntheses for an *N*-acyl-2-azetine and *N*-nitro-2-azetine, respectively. Barluenga and co-workers have recently reported the synthesis of an *N*-nosyl-2-azetine utilizing Cu catalysis.<sup>12</sup> After this paper was accepted and was undergoing review, *N*-acyl-2-azetines were reported to participate in a bioorthogonal reaction<sup>13</sup> with tetrazines.<sup>14</sup>

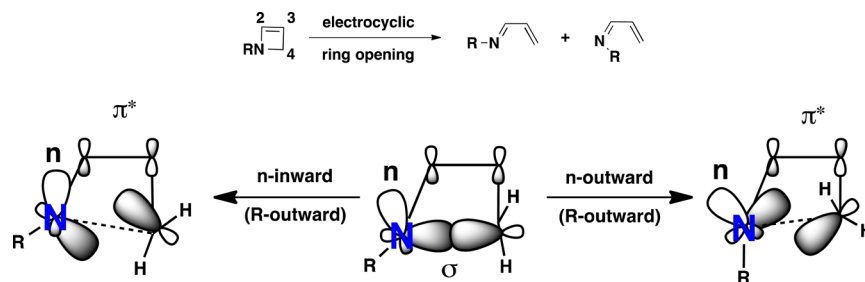
## COMPUTATIONAL METHODS

All computations were carried out with GAUSSIAN 09.<sup>15</sup> Reactants, transition states, and products were optimized with the density functional M06-2X<sup>16</sup> using the 6-31G+(d,p) basis set with an ultrafine grid.<sup>17</sup> M06-2X has been found to give more reliable energetics than B3LYP<sup>18</sup> for cycloadditions involving main group atoms.<sup>19</sup> Vibrational analysis confirmed all stationary points to be minima (no imaginary frequencies) or transition structures (one imaginary frequency). Thermal corrections were computed from unscaled frequencies for the standard state of 1 atm and 298.15 K. Truhlar’s quasiharmonic

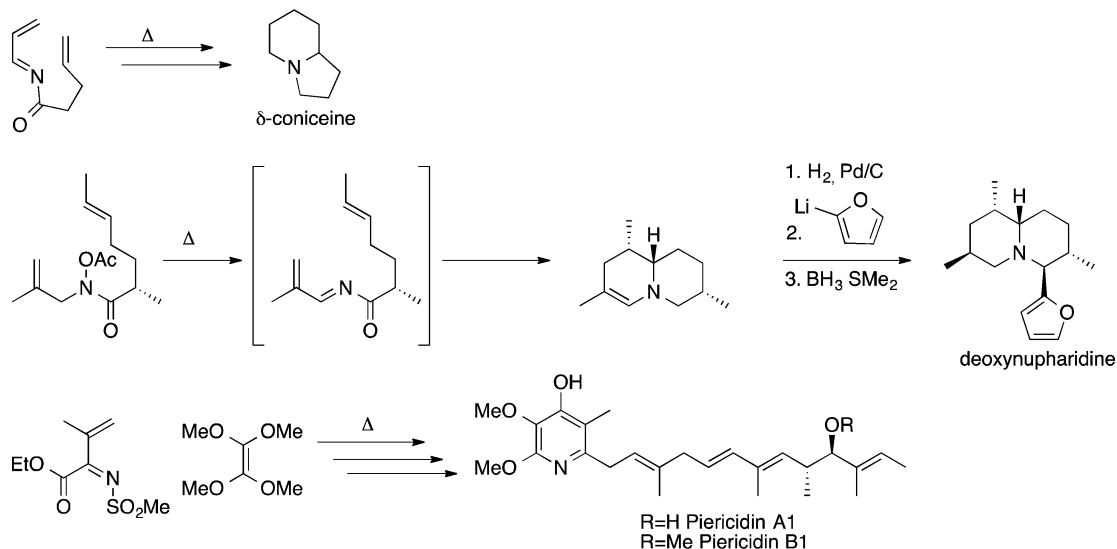
Received: April 25, 2014

Published: June 2, 2014

Scheme 1. Inward Rotation of the Lone Pair (n) on Nitrogen (Left). Outward Rotation of the Lone Pair on Nitrogen (Right)



Scheme 2. Natural Products Synthesized Using 1-Azadienes in Inverse-Electron-Demand Diels–Alder Reactions



correction was applied for entropy calculations by setting all frequencies to  $100\text{ cm}^{-1}$  when they are less than  $100\text{ cm}^{-1}$ .<sup>20,21</sup>

## RESULTS AND DISCUSSION

We first describe the effects of *N*-substituents on the geometries of 2-azetines. The structures of the following 2-azetines were computed for the following *N*-substituents: dimethylamino, methoxy, fluoro, chloro, trifluoromethyl, methyl, vinyl, cyano, acetyl, nitro, sulfonyl, and formyl. Figure 1 shows the optimized geometries for the series of 2-azetines studied here. The pyramidalization angle, defined as  $180^\circ$  minus the  $\text{C}_3\text{C}_2\text{NR}$  dihedral angle, is shown below each structure (Figure 1). This angle is  $55^\circ$  (half of  $109.5^\circ$ ) in a perfect tetrahedral geometry. The substituents are divided into three classes C, X, and Z as first defined by Houk.<sup>22</sup> These refer to conjugating groups (C), donors (X), and acceptors (Z), respectively.

The pyramidalization angle ranges from  $0$ – $61^\circ$ . With the exception of acyl groups, which prefer planar or almost planar geometries, other substituents do not differ substantially in the reactant geometry. Conjugating and strong  $\pi$  acceptors are able to delocalize the nitrogen lone pair, promoting planarization (e.g., 1-CHO).

## TRANSITION STRUCTURES

Both conrotatory transition structures were located for each of the *N*-substituted 2-azetines. Figures 2 and 3 show the lone-pair-in, substituent-out and lone-pair-out, substituent-in transition structures for the 2-azetines, respectively. These will be referred to as “out” and “in” transition structures, respectively, in the text.

The cyclobutene ring-opening transition structure can be found in both figures for comparison.

The breaking CN bond lengths are quite similar for these transition structures ( $1.96$ – $2.05\text{ \AA}$ ). As expected, CN bond lengths are shorter than the breaking CC bond length in the cyclobutene ring-opening reaction ( $2.14\text{ \AA}$ ). In the “out” transition states, *N*-substituents that can conjugate with the nitrogen lone pair retain planarity from reactant to transition state (e.g., TS-out-CHO, TS-out-NO<sub>2</sub>, TS-out-CN, TS-out-COMe). All of the transition structures are planarized relative to the reactant, with the exception of the *N*-acyl-2-azetines. 1-COMe and 1-CHO become more pyramidalized in the transition state because the nitrogen lone pair can delocalize into the CC  $\pi^*$  orbital. We did a Natural Bond Orbital analysis, (NBO version 3<sup>23</sup>) which indicated that the  $n_{\text{N}}-\pi^*_{\text{CC}}$  orbital interaction is the major donor (filled orbital) - acceptor (vacant orbital) interaction occurring. The  $n_{\text{N}}-\pi^*_{\text{CC}}$  orbital interaction is significantly higher for the “out” transition states than for the “in” transition states, because the nitrogen lone pair does not overlap with the  $\pi^*$  orbital in the “in” transition states. (Table S1, Supporting Information).

The transition structures where the *N*-substituent rotates inward are shown in Figure 3. These transition structures show the *N*-substituent rotated inward. The pyramidalization angles range from  $102$  to  $122^\circ$ . Overall, the transition structures with *N*-substituents that are donors have larger pyramidalization angles to minimize filled–filled orbital interactions with the breaking CN  $\sigma$  bond of the 2-azetines. The “in” transition structures also have similar  $\sigma$  bond-breaking distances ( $2.05$ – $2.12\text{ \AA}$ ),

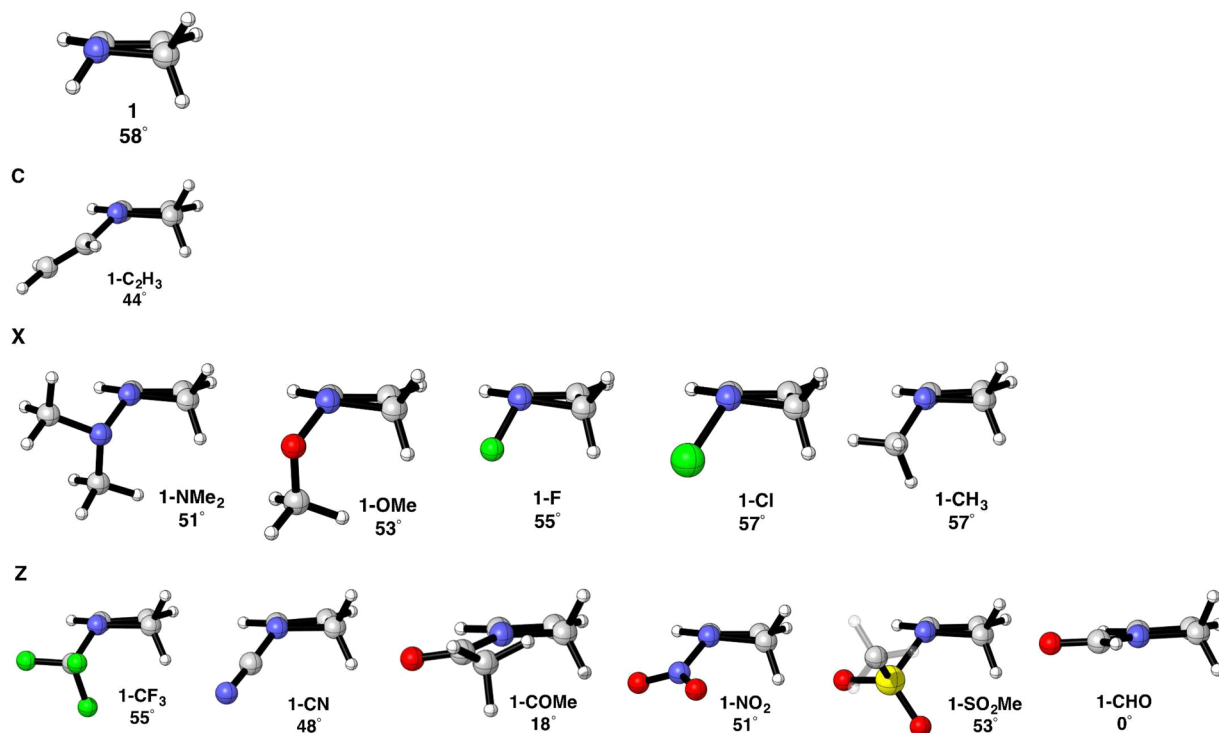


Figure 1. Optimized geometries of *N*-substituted 2-azetines (**1-R**). The pyramidalization angle is reported in degrees.

which are slightly longer than the “out” transition structures. The preference for the “out” transition structure ( $\Delta\Delta G^\ddagger$ ) shown in Figure 3 is largest for donor substituents and smallest for acceptors. This is related to the well-studied orbital interactions in electrocyclic ring-opening reactions of 3-substituted cyclobutenes.<sup>24</sup>

Three “out” transition structures for azetine ring-openings are overlaid with the transition structures of identically substituted 3-substituted-cyclobutenes and three “in” transition structures of *N*-substituted-2-azetines and 3-substituted cyclobutenes with the same substituents are overlaid in Figure 4.

Figure 4 demonstrates that the transition structures for *N*-substituted 2-azetines are nearly identical to the analogous 3-substituted cyclobutenes, except for a slight rotation of the acetyl group. This shows that the interaction of the substituent orbitals with the breaking  $\sigma$  bond (HOMO) are important for 2-azetines as well as cyclobutenes.

## REACTIVITY

The activation barriers for the transition structures shown in Figures 2 and 3 and the experimentally determined Taft  $\sigma_R^0$  parameters are shown in Table 1. The Taft  $\sigma_R^0$  parameter is an experimentally determined substituent constant that measures the resonance effect of the substituent.<sup>25</sup> The  $\pi$  donors have  $\sigma_R^0 < 0$  and  $\pi$  acceptors have  $\sigma_R^0 > 0$ . Table 1 is arranged from best donor to best acceptor according to  $\sigma_R^0$ .

The *N*-substituent prefers to rotate outward, while the nitrogen lone pair rotates inward, regardless of the *N*-substituent ( $\Delta G_{\text{out}}^\ddagger \ll \Delta G_{\text{in}}^\ddagger$ ). The activation free energies for outward rotation of the substituent strongly depend on the nature of the *N*-substituent: donors result in low activation barriers, while acceptors result in high barriers.  $\Delta G_{\text{out}}^\ddagger$  values range from 15.3 to 36.3 kcal mol<sup>-1</sup>, while the range of  $\Delta G_{\text{in}}^\ddagger$  values is more compressed: 38.7–48.7 kcal mol<sup>-1</sup>.

The large range of  $\Delta G_{\text{out}}^\ddagger$  is the result of reactant state stabilization of the 2-azetines. Delocalization of the lone pair with an acceptor (e.g., **1-CHO**) stabilizes the reactant, whereas donors destabilize the reactants because of a filled–filled orbital interaction between the nitrogen lone pair and the substituent (e.g., **1-F**). Destabilized reactants require the least amount of energy to reach the transition state, where the nitrogen lone pair is delocalized into the  $\pi^*$  orbital of the alkene. Stabilized reactants require more energy to reach the transition state; because the nitrogen lone pair can be delocalized into the acceptor orbital and the  $\pi_{\text{CC}}^*$ . This is demonstrated by plotting  $\Delta G_{\text{out}}^\ddagger$  with respect to  $\sigma_R^0$  (Figure 5).

Figure 5 shows a reasonably good ( $R^2 = 0.79$ ) linear relationship between  $\Delta G_{\text{out}}^\ddagger$  and  $\sigma_R^0$ . On the other hand, the correlation is poorer between  $\Delta G_{\text{in}}^\ddagger$  and  $\sigma_R^0$ ; the activation energy is high and only gradually decreases as the  $\pi$  acceptor character of the substituent increases. The data in Figure 5 were used to compute  $\rho$  values were computed from  $\log(k_{\text{R}}/k_{\text{H}})$  vs  $\sigma_R^0$  plots (Figures S1 and S2, Supporting Information). The  $\rho$  value for the “out” transition structures is  $-16.1$ . The very large magnitude and sign of  $\rho$  means that the reactivity is very sensitive to the character of the *N*-substituent. There is no significant charge difference from reactant to transition state, but in reactants, the substituents interact strongly with the lone pair on nitrogen and in the transition state mainly with the  $\sigma_{\text{CN}}^*$  acceptor orbital of the breaking bond. The  $\rho$  value for the “in” transition structures is 3.6, which indicates low sensitivity to the *N*-substituent and a small increase in the interaction with the nitrogen lone pair in the transition state.

The relationship of reactivity and  $\sigma_R^0$  was compared to that of the frequently studied ring-opening reaction of 3-substituted-cyclobutenes.<sup>19</sup> We computed the activation free energies for the ring-opening reaction (geometries and energies in the Supporting Information) with the same methods used for the azetines. A plot of  $\Delta G_{\text{out}}^\ddagger$  or  $\Delta G_{\text{in}}^\ddagger$  vs  $\sigma_R^0$  is shown in Figure 6 to

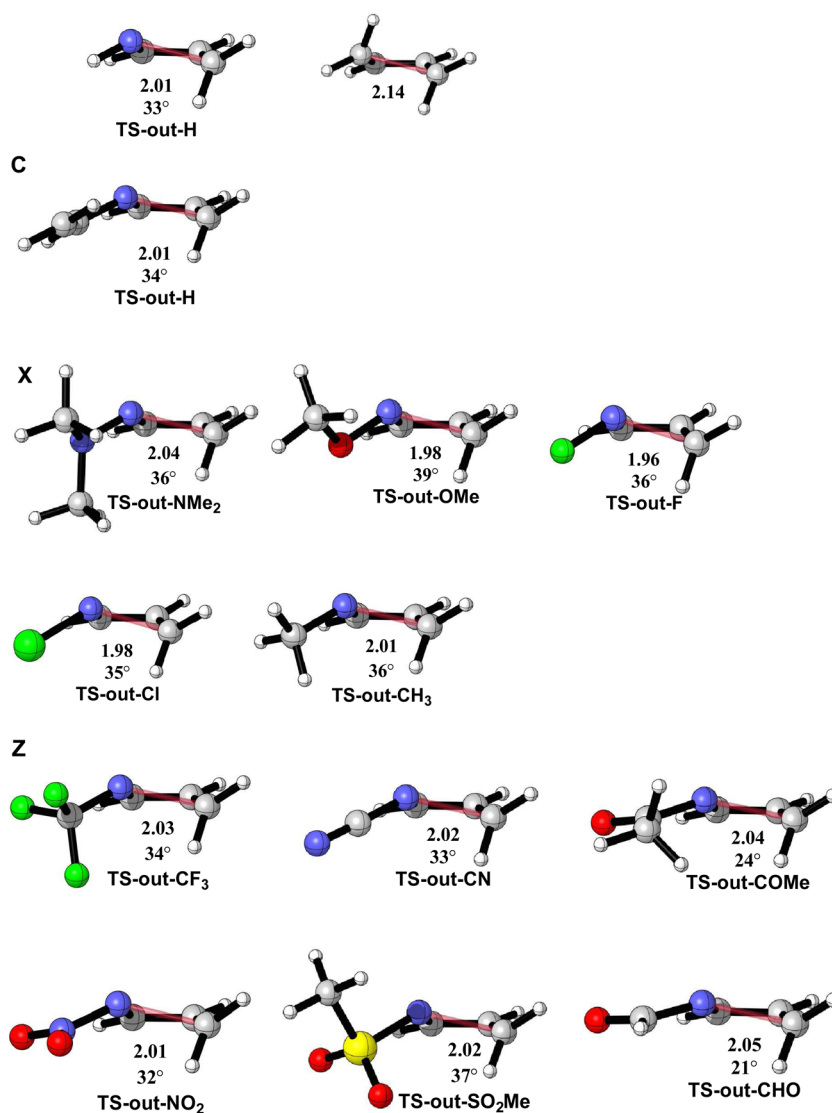


**Figure 2.** Electro-cyclic conrotatory ring-opening lone-pair-in, substituent-out transition structures. Breaking CC or CN bond lengths are reported in angstroms. The pyramidalization angle is reported in degrees.

evaluate the sensitivity of the reactivity of 3-substituted cyclobutenes to the nature of the substituent.

Previous calculations established that  $\Delta G_{\text{in}}^{\ddagger} - \Delta G_{\text{out}}^{\ddagger}$  correlates well with  $\sigma_{\text{R}}^0$ . In Figure 6, the  $\Delta G_{\text{in}}^{\ddagger}$  and  $\Delta G_{\text{out}}^{\ddagger}$  are plotted individually for cyclobutenes. The  $\rho$  values were computed for the 3-substituted cyclobutene cases shown in Figure 6 (Figures S3 and S4, Supporting Information). The magnitude of  $\rho$  is lower for the carbocyclic ring-opening than for that the “out” transition structures of 2-azetines ( $\rho = -9.1$  vs  $-16.1$ , respectively). The  $\rho$  value for the “in” transition states is 6.1, but the correlation is very poor. The difference in  $\rho$  is due to the direct resonance interaction between the substituent and the nitrogen lone pair. This interaction is not possible in the carbocyclic cases and only the substituent stabilization of the breaking  $\sigma$  bond remains. Donors favor outward rotation substantially by interaction with the  $\sigma_{\text{CC}}^*$  orbital of the breaking bond, while there is no clear trend for inward rotation due to substantial closed shell repulsion for donors that is overridden by acceptor stabilization upon inward rotation.

Inward rotation of the *N*-substituent causes the lone pair to rotate outward, where it cannot interact with the  $\pi^*$  LUMO of the azetine. Reactivity gradually increases as the substituent

changes from a strong donor to a strong acceptor. The poor correlation between  $\Delta G_{\text{in}}^{\ddagger}$  and  $\sigma_{\text{R}}^0$  for cyclobutenes is consistent with a previous study where we established that even strong acceptors (e.g.,  $\text{NO}_2$ ) prefer to rotate outward for 3-substituted cyclobutenes.<sup>24h</sup> Competing steric and electronic effects in the transition states erodes the preference for “in” transition structures for cyclobutenes and 2-azetines substituted with acceptors. A plot of  $\Delta G_{\text{in}}^{\ddagger} - \Delta G_{\text{out}}^{\ddagger}$  for cyclobutene ring-opening and  $\sigma_{\text{R}}^0$  is shown in Figure 7.

Although the correlation of  $\Delta G_{\text{in}}^{\ddagger} - \Delta G_{\text{out}}^{\ddagger}$  with  $\sigma_{\text{R}}^0$  is relatively good for the 3-substituted cyclobutenes, the correlation of individual values of  $\Delta G_{\text{in}}^{\ddagger}$  and  $\Delta G_{\text{out}}^{\ddagger}$  with  $\sigma_{\text{R}}^0$  is poor. This was previously shown by our group,<sup>24h</sup> and we now find a nearly identical relationship between  $\Delta G_{\text{in}}^{\ddagger} - \Delta G_{\text{out}}^{\ddagger}$  and  $\sigma_{\text{R}}^0$  for *N*-substituted 2-azetines. Figure 7 shows a larger  $R^2$  value for the 2-azetines, likely due to the increased resonance interaction between the substituent and nitrogen lone pair, relative to the cyclobutene cases. The role of reactant stabilization on reactivity was further assessed by calculating the reaction free energies for the conversion of 2-azetines to 1-azadienes. Table 2 shows the reaction energies corresponding to 2-out-(a-m) and 2-in-(a-m).

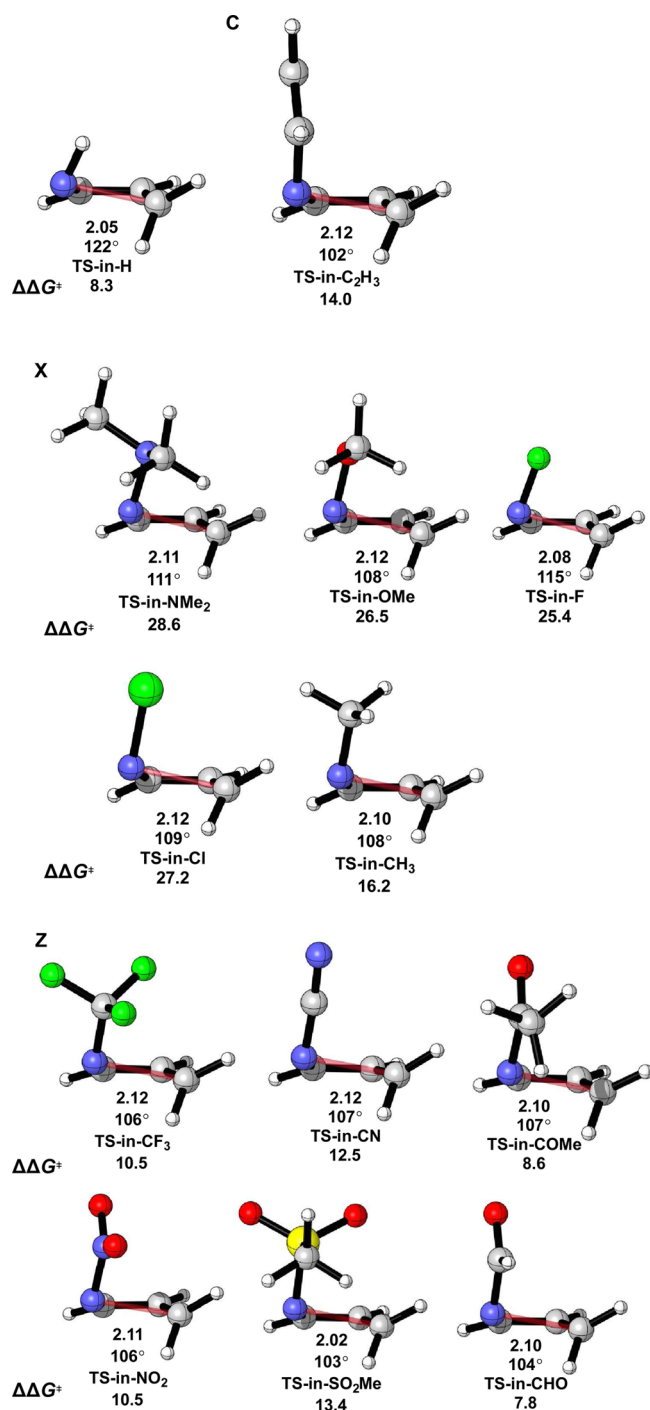


**Figure 3.** Electrocyclic conrotatory ring-opening lone-pair-out, substituent-in transition structures. Breaking CC or CN bond lengths are reported in angstroms. The pyramidalization angle is reported in degrees. The energies of these transition structures to that of the outward rotation (Figure 2) are given in kcal mol<sup>-1</sup> and are shown below each structure.

Table 2 shows that the reaction free energies corresponding to **2-out-(a-m)** and **2-in-(a-m)** are all exergonic [(-9.5 to -28.3 kcal mol<sup>-1</sup>) and (-7.0 to -27.7 kcal mol<sup>-1</sup>)], respectively. The *trans*-1-azadienes resulting from outward rotation are all more stable than the *cis* cases. When the *N*-substituent is a  $\pi$  acceptor, the reactant is stabilized and the reaction free energies are least exergonic for the formation of **2-out-(a-m)** and **2-in-(a-m)** [(-9.5 to -19.1 kcal mol<sup>-1</sup>) and (-7.0 to -17.4 kcal mol<sup>-1</sup>)].  $\pi$

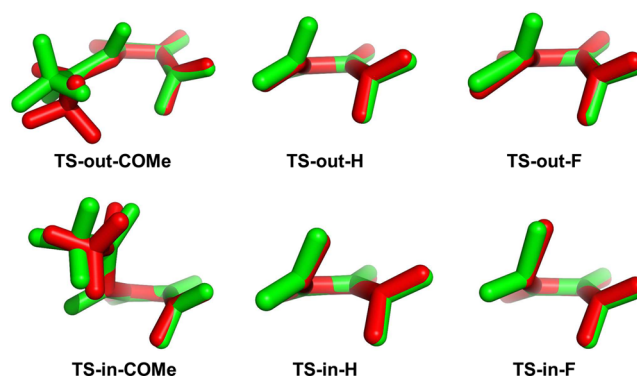


**Figure 4.** Overlaid “out” and “in” transition structures are shown in the top and bottom rows, respectively, for selected *N*-substituted 2-azetines (red) and 3-substituted cyclobutenes (green).

**Table 1.** Activation Free Energies for Both Diastereomeric Transition Structures of the Electrocyclic Ring-Opening Reactions of Azetines<sup>a</sup>

<i>N</i> -R	$\Delta G_{\text{out}}^\ddagger$	$\Delta G_{\text{in}}^\ddagger$	$\sigma_{\text{R}}^0$	<i>N</i> -R	$\Delta G_{\text{out}}^\ddagger$	$\Delta G_{\text{in}}^\ddagger$	$\sigma_{\text{R}}^0$
NMe <sub>2</sub>	18.3	46.9	-0.56	CF <sub>3</sub>	32.2	42.7	0.10
OMe	15.3	41.8	-0.43	CN	27.5	40.1	0.13
F	20.9	46.3	-0.34	COMe	35.4	44.0	0.16
Cl	21.5	48.7	-0.23	NO <sub>2</sub>	30.0	44.8	0.16
CH <sub>3</sub>	29.5	45.7	-0.13	SO <sub>2</sub> Me	27.9	41.3	0.19
C <sub>2</sub> H <sub>3</sub>	29.2	43.2	-0.01	CHO	36.3	44.1	0.23
H	30.4	38.7	0				

<sup>a</sup> The activation barriers are given in kcal mol<sup>-1</sup>.  $\Delta G_{\text{out}}^\ddagger$  and  $\Delta G_{\text{in}}^\ddagger$  refer to the activation barriers corresponding to transition structures where the *N*-substituent rotates outward or inward.

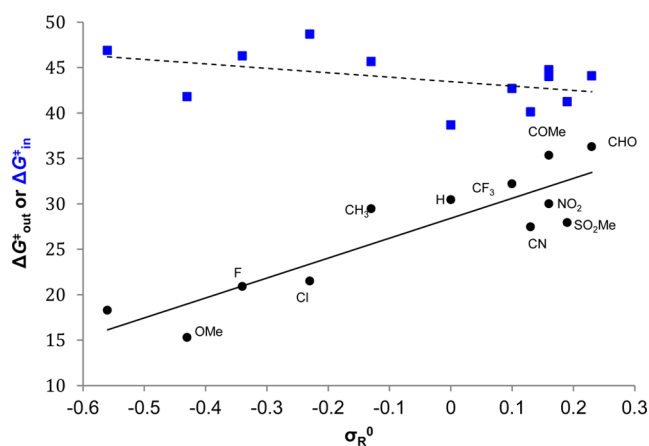


**Figure 5.** Computed  $\Delta G_{\text{out}}^\ddagger$  (black circles) and  $\Delta G_{\text{in}}^\ddagger$  (blue squares) plotted against the Taft  $\sigma_{\text{R}}^0$  parameter.  $\Delta G_{\text{out}}^\ddagger = 21.9\sigma_{\text{R}}^0 + 28.4$ ;  $R^2 = 0.79$ .  $\Delta G_{\text{out}}^\ddagger$  corresponds to lone-pair-in, substituent-out.  $\Delta G_{\text{in}}^\ddagger = -4.9\sigma_{\text{R}}^0 + 43.4$ ;  $R^2 = 0.20$ .  $\Delta G_{\text{in}}^\ddagger$  refers to lone-pair-out, substituent-in.

Donor substituents result in more exergonic reactions for **2-out-(a-m)** and **2-in-(a-m)** [(-17.5 to -28.3 kcal mol<sup>-1</sup>) and (-17.5 to -27.7 kcal mol<sup>-1</sup>)]. Figure 8 shows plots of  $\Delta G_{\text{out}}^\ddagger$  vs  $\Delta G_{\text{out}}$  and  $\Delta G_{\text{in}}^\ddagger$  vs  $\Delta G_{\text{in}}$  for the ring-opening reactions of *N*-substituted-2-azetines to evaluate the relationship between reactivity and reaction energies for both modes of conrotatory ring-opening reactions.

Figure 8 shows that for outward rotation, the reaction energy varies significantly as the *N*-substituent are changed. The

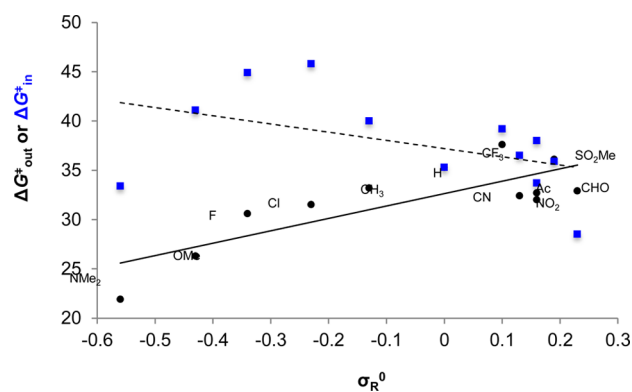


**Figure 6.** Computed  $\Delta G_{\text{out}}^{\ddagger}$  (black circles) and  $\Delta G_{\text{in}}^{\ddagger}$  (blue squares) plotted against Taft  $\sigma_{\text{R}}^0$  for the ring-opening reaction of 3-substituted cyclobutenes.  $\Delta G_{\text{out}}^{\ddagger} = 12.6\sigma_{\text{R}}^0 + 32.6$ ;  $R^2 = 0.64$ .  $\Delta G_{\text{out}}^{\ddagger}$  is for outward rotation of the substituent.  $\Delta G_{\text{in}}^{\ddagger} = -8.3\sigma_{\text{R}}^0 + 37.2$ ;  $R^2 = 0.21$ .  $\Delta G_{\text{in}}^{\ddagger}$  is for inward rotation of the substituent.

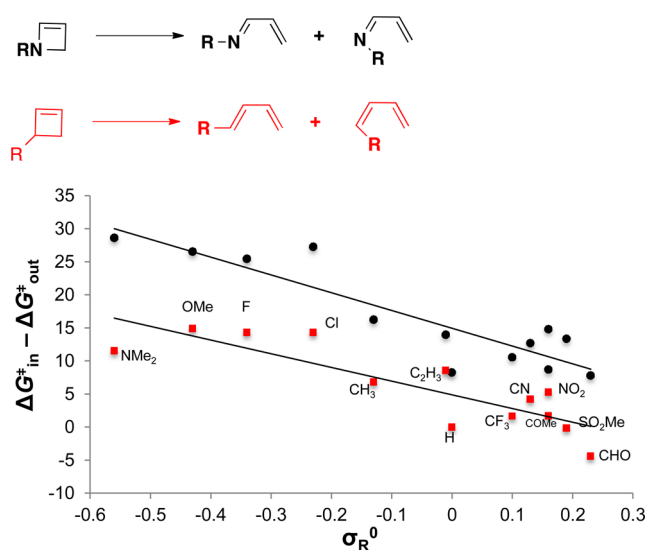


**Figure 7.** Activation barrier difference plotted against Taft  $\sigma_{\text{R}}^0$  values for the electrocyclic ring-opening of 3-substituted cyclobutenes (red squares) and *N*-substituted-2-azetines (black circles). The linear regression equations are  $\Delta G_{\text{in}}^{\ddagger} - \Delta G_{\text{out}}^{\ddagger} = -20.7\sigma_{\text{R}}^0 + 4.9$ ;  $R^2 = 0.73$  and  $\Delta G_{\text{in}}^{\ddagger} - \Delta G_{\text{out}}^{\ddagger} = -26.9\sigma_{\text{R}}^0 + 15.0$ ;  $R^2 = 0.82$ , respectively.

**Table 2.** Reaction Energies for the Ring-Opening Reactions of 2-Azetines<sup>a</sup>

<i>N</i> -R	$\Delta G_{\text{out}}$	$\Delta G_{\text{in}}$	<i>N</i> -R	$\Delta G_{\text{out}}$	$\Delta G_{\text{in}}$
NMe <sub>2</sub>	-24.4	-18.7	CF <sub>3</sub>	-16.2	-10.0
OMe	-28.3	-27.7	CN	-19.1	-17.4
F	-21.6	-17.5	COMe	-10.9	-8.1
Cl	-19.8	-16.9	NO <sub>2</sub>	-13.8	-10.9
CH <sub>3</sub>	-19.4	-14.8	SO <sub>2</sub> Me	-17.4	-7.4
C <sub>2</sub> H <sub>5</sub>	-19.3	-14.5	CHO	-9.5	-7.0
H	-18.8	-17.5			

<sup>a</sup>Energy values reported in kcal mol<sup>-1</sup>.

activation free energies corresponding to the “in” transition structures do not depend on the reaction energies because the substituent influences the reactant and transition state energies similarly.

Donors destabilize *N*-substituted 2-azetines, effectively decreasing the energy required to reach the transition state.

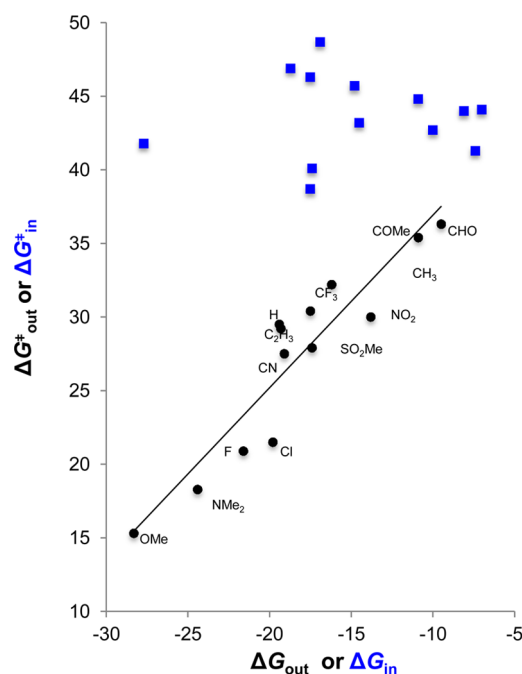


**Figure 8.** Computed  $\Delta G_{\text{out}}^{\ddagger}$  (black circles) and  $\Delta G_{\text{in}}^{\ddagger}$  (blue squares) plotted against  $\Delta G_{\text{out}}$  or  $\Delta G_{\text{in}}$  for the ring-opening of 2-azetines.  $\Delta G_{\text{out}}^{\ddagger} = 1.17\Delta G_{\text{out}} + 48.6$ ;  $R^2 = 0.86$ .  $\Delta G_{\text{out}}^{\ddagger}$  corresponds to the substituent rotating outward.  $\Delta G_{\text{in}}^{\ddagger} = 0.01\Delta G_{\text{in}} + 43.9$ ;  $R^2 = 0.00$ .  $\Delta G_{\text{in}}^{\ddagger}$  refers to the substituent rotating inward.

The reaction energies are more negative when the substituent is a  $\pi$  donors. Acceptors stabilize 2-azetines by delocalizing the nitrogen lone pair, which corresponds to higher activation free energies and reduced exergonicities.

## CONCLUSION

The origins of the torquoselectivities and reactivities of the electrocyclic ring-opening reactions of 2-azetines were determined. The lone-pair-in, substituent-out transition structures are always lower in energy than the lone-pair-in, substituent-out transition structures. The torquoselectivities for these reactions result from the interaction of the nitrogen lone pair with the  $\pi^*$  orbital of the 2-azetine ( $n_{\text{N}}-\pi_{\text{CC}}^*$ ) upon outward rotation of the substituent. The energies of 2-azetines are strongly affected by the nature of the *N*-substituent. A linear correlation was found to exist between  $\Delta G^{\ddagger}$  and  $\Delta G_{\text{rxn}}$  for the “out” transition structures. Acceptors stabilize the reactant state by delocalizing the nitrogen lone pair, while donors destabilize the reactant state due to unfavorable filled–filled orbital interactions. The transition structures are much less sensitive to the nature of the *N*-substituent and the large range of activation free energies depends on the reactant state energies of the 2-azetines. Further computational studies regarding the utility of substituted 2-azetines as chemical reporters in bioorthogonal reactions are ongoing.

## ASSOCIATED CONTENT

### Supporting Information

Calculated geometries and corresponding energies. This material is available free of charge via the Internet at <http://pubs.acs.org>.

## AUTHOR INFORMATION

### Corresponding Author

\*E-mail: [houk@chem.ucla.edu](mailto:houk@chem.ucla.edu).

## Notes

The authors declare no competing financial interest.

## ACKNOWLEDGMENTS

We thank Ashay Patel and Martin Breugst for helpful comments and the National Science Foundation (NSF CHE-1059084) for financial support of this research. Calculations were performed on the Hoffman2 cluster at UCLA and the Extreme Science and Engineering Discovery Environment (XSEDE), which is supported by National Science Foundation Grant No. OCI-10535. Figures 1–3 were generated using CYLview.<sup>26</sup>

## REFERENCES

- (1) (a) Woodward, R. B.; Hoffmann, R. *J. Am. Chem. Soc.* **1965**, *87*, 395. (b) Vogel, E. *Angew. Chem.* **1954**, *66*, 640.
- (2) (a) Kirmse, W.; Rondan, N. G.; Houk, K. N. *J. Am. Chem. Soc.* **1984**, *106*, 7989. (b) Rondan, N. G.; Houk, K. N. *J. Am. Chem. Soc.* **1985**, *107*, 2099.
- (3) Walker, M.; Hietbrink, B. N.; Thomas, B. E., IV; Nakamura, K.; Kallel, E. A.; Houk, K. N. *J. Org. Chem.* **2001**, *66*, 6669.
- (4) Jaccob, M.; Jem, I. S.; Giri, S.; Venuvanalingam, P.; Chattaraj, P. K. *J. Phys. Org. Chem.* **2011**, *24*, 460.
- (5) Zhou, Z.; Parr, R. G. *J. Am. Chem. Soc.* **1990**, *112*, 5720.
- (6) Manginck, S.; Speybroeck, V. V.; Vansteenkiste, P.; Waroquier, M.; de Kimpe, N. *J. Org. Chem.* **2008**, *73*, 5481.
- (7) Monbaliu, J.-C. M.; Masschelein, K. G. R.; Stevens, C. V. *Chem. Soc. Rev.* **2011**, *40*, 4708.
- (8) Jung, M. E.; Choi, Y. M. *J. Org. Chem.* **1991**, *56*, 6729.
- (9) Schnermann, M. J.; Boger, D. L. *J. Am. Chem. Soc.* **2005**, *127*, 15704.
- (10) Ma, C.; Gu, J.; Teng, B.; Zhou, Q.-Q.; Li, R.; Chen, Y.-C. *Org. Lett.* **2013**, *15*, 6206.
- (11) Marchand, A. P.; Rajagopal, D.; Bott, S. G.; Archibald, T. G. *J. Org. Chem.* **1994**, *59*, 1608.
- (12) Barluenga, J.; Riesgo, L.; Lonzi, G.; Tomas, M.; Lopez, L. A. *Chem.—Eur. J.* **2012**, *18*, 922.
- (13) Debets, M. F.; v. Hest, J. C. M.; Rutjes, F. P. J. T. *Org. Biomol. Chem.* **2013**, *11*, 6439 and references cited therein.
- (14) Engelsma, S. B.; Willems, L. I.; v. Paaschen, C. E.; v. Kasteren, S. I.; van der Marel, G. A.; Overkleeft, H. S.; Filippov, D. V. *Org. Lett.* **2014**, *16*, 2744.
- (15) Frisch, M. J.; Trucks, G. W.; Schlegel, H. B.; Scuseria, G. E.; Robb, M. A.; Cheeseman, J. R.; Scalmani, G.; Barone, V.; Mennucci, B.; Petersson, G. A.; Nakatsuji, H.; Caricato, M.; Li, X.; Hratchian, H. P.; Izmaylov, A. F.; Bloino, J.; Zheng, G.; Sonnenberg, J. L.; Hada, M.; Ehara, M.; Toyota, K.; Fukuda, R.; Hasegawa, J.; Ishida, M.; Nakajima, T.; Honda, Y.; Kitao, O.; Nakai, H.; Vreven, T.; Montgomery, J. A., Jr.; Peralta, J. E.; Ogliaro, F.; Bearpark, M.; Heyd, J. J.; Brothers, E.; Kudin, K. N.; Staroverov, V. N.; Kobayashi, R.; Normand, J.; Raghavachari, K.; Rendell, A.; Burant, J. C.; Iyengar, S. S.; Tomasi, J.; Cossi, M.; Rega, N.; Millam, J. M.; Klene, M.; Knox, J. E.; Cross, J. B.; Bakken, V.; Adamo, C.; Jaramillo, J.; Gomperts, R.; Stratmann, R. E.; Yazyev, O.; Austin, A. J.; Cammi, R.; Pomelli, C.; Ochterski, J. W.; Martin, R. L.; Morokuma, K.; Zakrzewski, V. G.; Voth, G. A.; Salvador, P.; Dannenberg, J. J.; Dapprich, S.; Daniels, A. D.; Farkas, O.; Foresman, J. B.; Ortiz, J. V.; Cioslowski, J.; Fox, D. J. *Gaussian 09*, revision C.01; Gaussian Inc.: Wallingford, CT, 2010.
- (16) Zhao, Y.; Truhlar, D. G. *Theor. Chem. Acc.* **2008**, *120*, 215.
- (17) Wheeler, S. E.; Houk, K. N. *J. Chem. Theory Comput.* **2010**, *6*, 395.
- (18) (a) Becke, A. D. *J. Chem. Phys.* **1993**, *98*, 5648. (b) Stephens, P. J.; Devlin, F. J.; Chabalowski, C.; Frisch, M. J. *J. Phys. Chem.* **1994**, *98*, 11623.
- (19) Zhao, Y.; Truhlar, D. G. *Acc. Chem. Res.* **2008**, *41*, 157.
- (20) Zhao, Y.; Truhlar, D. G. *Phys. Chem. Chem. Phys.* **2008**, *10*, 2813.
- (21) Ribeiro, R. F.; Marenich, A. V.; Cramer, C. J.; Truhlar, D. G. *J. Phys. Chem. B* **2011**, *115*, 14556.
- (22) Houk, K. N. *J. Am. Chem. Soc.* **1973**, *95*, 4092.
- (23) NBO Version 3.1, Glendening, E. D.; Reed, A. E.; Carpenter, J. E.; Weinhold, F.; .
- (24) (a) Rudolf, K.; Spellmeyer, D. C.; Houk, K. N. *J. Org. Chem.* **1987**, *52*, 3708. (b) Houk, K. N.; Spellmeyer, D. C.; Jefford, C. W.; Rimbault, C. G.; Wang, Y.; Miller, R. D. *J. Org. Chem.* **1988**, *53*, 2125. (c) Buda, A. B.; Wang, Y.; Houk, K. N. *J. Org. Chem.* **1989**, *54*, 2264. (d) Kallel, E. A.; Wang, Y.; Spellmeyer, D. C.; Houk, K. N. *J. Am. Chem. Soc.* **1990**, *112*, 6759. (e) Niwayama, S.; Houk, K. N. *Tetrahedron Lett.* **1992**, *33*, 883. (f) Nakamura, K.; Houk, K. N. *Heterocycles* **1993**, *35*, 631. (g) Evanseck, J. D.; Thomas, B. E., IV; Spellmeyer, D. C.; Houk, K. N. *J. Org. Chem.* **1995**, *60*, 7134. (h) Niwayama, S.; Kallel, E. A.; Spellmeyer, D. C.; Sheu, C.; Houk, K. N. *J. Org. Chem.* **1996**, *61*, 2813. (i) Niwayama, S.; Kallel, E. A.; Sheu, C.; Houk, K. N. *J. Org. Chem.* **1996**, *61*, 2517. (j) Dolbier, W. R., Jr.; Koroniak, H.; Houk, K. N.; Sheu, C. *Acc. Chem. Res.* **1996**, *29*, 471. (k) *J. Am. Chem. Soc.* **1992**, *114*, 1157. (l) Matsuya, Y.; Ohsawa, N.; Hideo, N. *J. Am. Chem. Soc.* **2006**, *128*, 412. (m) Ibrahim-O, M. *Tetrahedron Lett.* **2010**, *51*, 3610.
- (25) Taft, R. W.; Lewis, I. C. *J. Am. Chem. Soc.* **1958**, *80*, 2436.
- (26) Legault, C. Y. CYLview 1.0b; Université de Sherbrooke; 2014 ([www.cylview.org](http://www.cylview.org)).